01 Nov 2002

Numerical Simulation of Partial Discharge Propagation in Cable Joints using the Finite Difference Time Domain Method

David Pommerenke
Missouri University of Science and Technology, davidjp@mst.edu

R. Jobava

R. Heinrich

Numerical Simulation of Partial Discharge Propagation in Cable Joints Using the Finite Difference Time Domain Method

Key Words: Partial discharge (PD) propagation, cable joint models, finite difference time domain (FDTD) method, PD location, PD sensors, calibration

D. Pommerenke
University of Missouri-Rolla

R. Jobava
Tbilisi State University
Tbilisi, Georgia

R. Heinrich
Technical University of Berlin

In the previous article in this series [1], we discussed the simulation of PD propagation through electromagnetic modeling. Continuing this series, we report on the PD propagation and detection in cable joints.

A cascade of breakdowns in a series of 150 kV terminations on one day in 1993 caused a major blackout in the Netherlands [2] and recently, some 240 kV cable joints failed in Singapore. In almost every case, PD is a predecessor to breakdown of polymer insulation. Using sensitive PD detection that distinguishes between external noise and internal PD, defects can often be detected during field testing, prior to breakdown. Capacitive, inductive, galvanic, or directional coupling methods are available for sensing PD [3]-[5].

Criteria for choosing a sensing method include sensitivity and the ability to distinguish noise from PD. This article compares sensing principles based on the use of electromagnetic simulation of PD propagation in a cable joint.

Criteria for choosing a sensing method include sensitivity and the ability to distinguish noise from PD.

The propagation of pulses in cables can be simulated using equivalent circuit models [6]. However, as a result of the complex nature of cable joints, such an analysis cannot be carried out with sufficient accuracy by equivalent circuits or analytically as for gas-insulated switchgear (GIS) [7]. Instead, a numerical electromagnetic method (FDTD) is applied. This facilitates determining through computation the output signal of the sensors for various PD locations within the cable joint, a task that would be very difficult and time consuming by experimental methods.

Cable Joint Modeled

The cable joint [8]-[9] being modeled is a silicone rubber 110 kV slip-on joint made by Pirelli for 500 mm^2 (1000 kcmil) conductors. The splice body is 865 mm (35 inches) long by 172 mm (7 inches) in diameter and is part of a cable joint family extending to 550 kV. A longitudinal cross section is shown in Fig. 1.

The manufacturer provided the dielectric constants for cross-linked polyethylene (XLPE) and silicone rubber, see Table I. The values for the epoxy are within the typical range ($e_r = 4 - 5$). The dielectric parameters of the conductive silicone rubber needed to be treated with care, as the FDTD algorithm used here did not accommodate the strong frequency dependence of the permittivity. The permittivity of the conductive silicone rubber was adjusted for the best match between the simulated and measured results for a pulse that travels through the cable joint. In this way, an "effective" permittivity was obtained. Given the short lengths of the high-voltage cables at either end of the cable joint in the numerical model, the cable semiconducting layers have little influence on the PD pulse (<1 dB). Data on typical values can be found in [10]-[11]. The simulation was validated by the methods shown in [1]. As the computational model is not valid above 400 MHz, all data were low-pass filtered at 300 MHz. The Fidelity FDTD code was used in this effort [12].

Comparison of Cable Joint PD Sensors

The sensors investigated through electromagnetic simulation are shown in Fig. 2. Each sensor was optimized through numerical simulation.

- Configuration A is based on [13]. Two capacitive electrodes are used.
- Configuration B is similar to the one used in the BEWAG prequalification of 400 kV XLPE cables at CESI and uses one large electrode around the joint.
- Configuration C has been derived from A. It uses 360° electrodes to reduce the effect of the azimuthal PD location.
- Configuration D uses two longitudinal electrodes. Noise that travels along the cable is suppressed by differential amplification of the potential between the electrodes.
- Configuration E uses electrodes on either side of the joint for directional coupling [5].

PD Locations

Although PD can occur at almost any location within the cable joint, the field distribution and practical experience guided the location of the PD sources (Fig. 3). The interface between the XLPE of the cable and the silicone rubber (location 3) is critical, as it is stressed by a parallel electric field and is mounted on site. PD at this interface has caused a number of breakdowns [2]. The largest field strength occurs at the edge of the conductor connection shield (location 1). Location 4 simulates a faulty outer semicon layer.

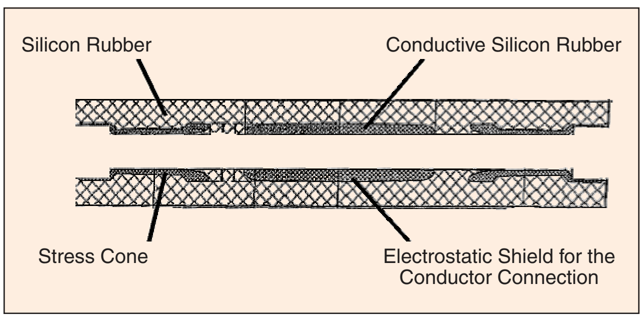

Figure 1. Longitudinal cross-section of a 110 kV silicone rubber slip-on cable joint shown without the cable. It was simulated in a through, not in a cross over, configuration.

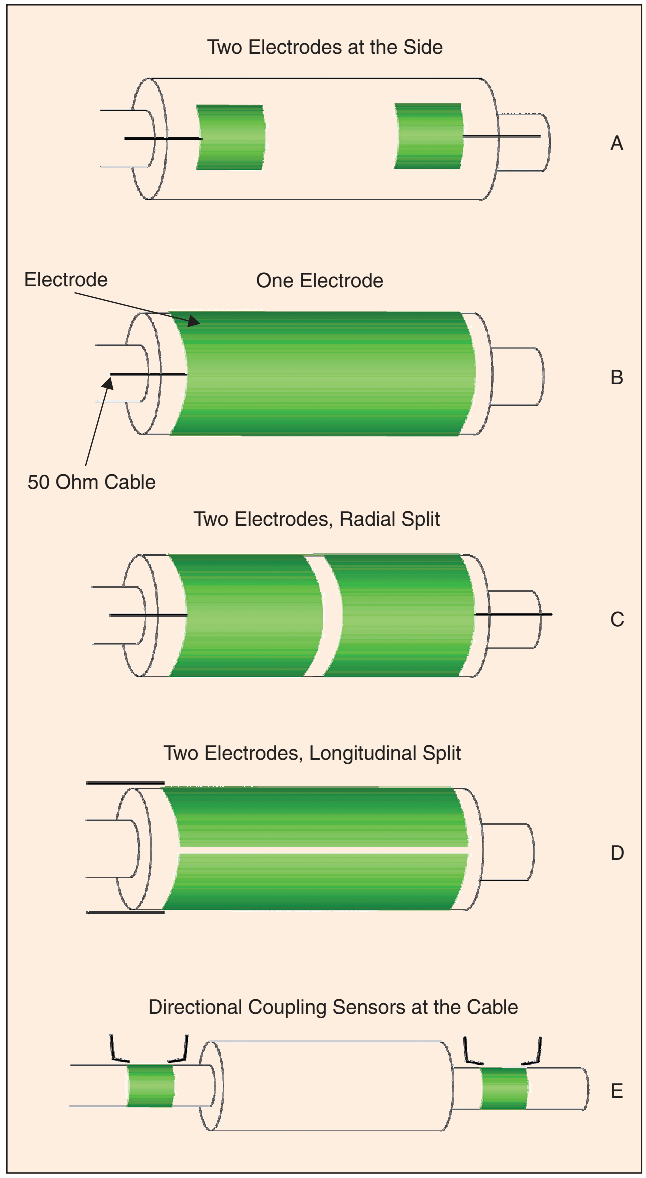

Figure 2. Configuration of PD sensing electrodes attached to the cable joint.

Table I. Dielectric Parameter Used for Modeling the Cable Joint		
	Epsilon	Conductivity [S/m]
Cable XLPE	2.3	0
Semicon of the cable	30.0	2
Silicone rubber	3.2	0
Conductive silicone rubber	90.0	0.5
Epoxy	5.0	0.0055

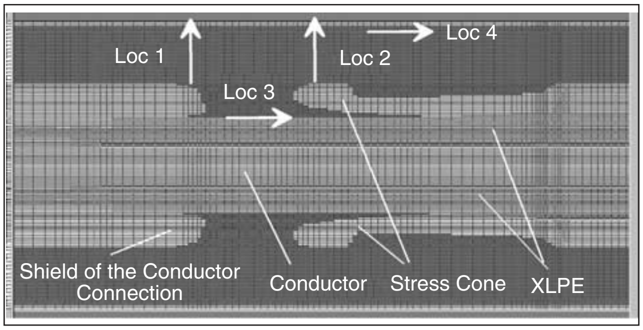

Figure 3. Locations of the simulated PD.

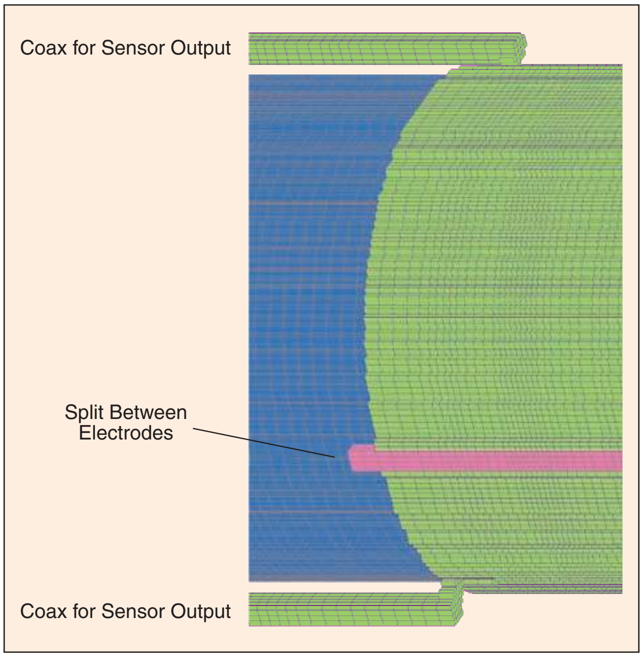

Figure 4. Detail of the output coax cables and the split for sensor configuration D. To provide better visibility of the inner sensor structure, the outer joint elements are not shown.

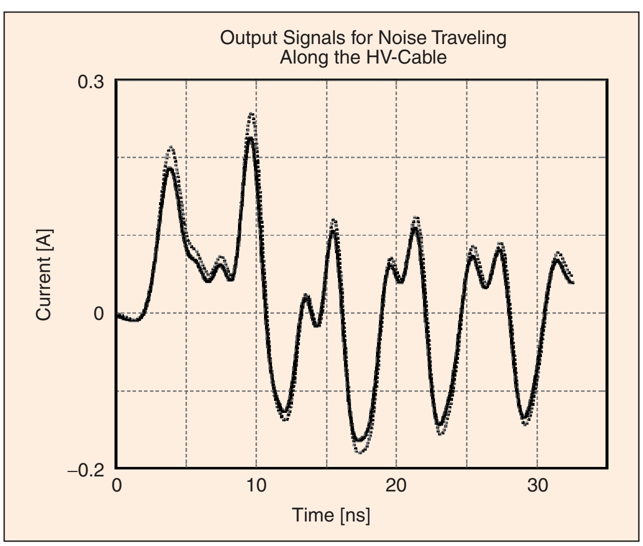

Figure 5. Signals at the two electrodes for a pulse that travels along the cable. Differential amplification of these signals will suppress such interference.

For sensor style A, the PDs were close to the sensor and 180° away from the sensing electrode ("crossed") leading to a total of 8 PD locations.

Configuration D was treated in a similar fashion. To test the influence of symmetry on the sensor output signals, the PD source was located within the plane of the electrode split (configuration D) and 90° from it.

Obviously, PD can occur in an infinite number of locations. Showing that a sensor maintains reasonable sensitivity for all the PD locations investigated does not prove that it will work for all possible locations. But lack of sensitivity at one of the PD locations investigated is sufficient to rule out a sensor.

As excitation, a Gaussian-shaped current pulse was used with a bandwidth of 500 MHz (FWHH of 0.6 ns). As a current is forced within nonconducting media, an electrostatic field is established by the pulse, as space charge will be left after the current flow ceases. This is similar to having the first PD in a space-charge free dielectric driven by an external electric field.

Results

In the following, some typical results are discussed; more details can be found in [9]. Sensor configuration D is based on the differential signal from the electrodes in order to suppress the signal from pulses that travel along the cable. If pure symmetry were maintained, detection of PD in all locations would not be possible. For that reason, the symmetry was broken by offsetting the output coax cables (see Fig. 4).

If a signal travels along the cable, both output signals are very similar (Fig. 5), and interference from such signals is suppressed through differential amplification. However, the question remains whether a PD signal will be detected from all 8 PD locations investigated. Two locations are shown in Fig. 6, both of which are along the interface between the XLPE and the silicone rubber. The output signals are shown in Fig. 7. While a PD at location A would produce a good difference signal, the signal would be much smaller for PD at location B and might be taken as residual noise from pulses propagating down the cable.

Estimation of the PD Location

With the knowledge of the propagation velocity through the cable joint and the time delay between the signals observed to the left and to the right of a cable joint, an estimate of the PD location can be given. The accuracy of such an estimate can be evaluated by simulation.

Figure 8(a) shows the currents to the left and right of the cable joint for PD location 2 (Fig. 3). Given that the average electromagnetic propagation velocity in the cable is 0.53 that of the speed of light and the measured PD delay is 2.6 ns, the estimated PD location is quite close to the actual PD source. But this picture changes if PD loca-

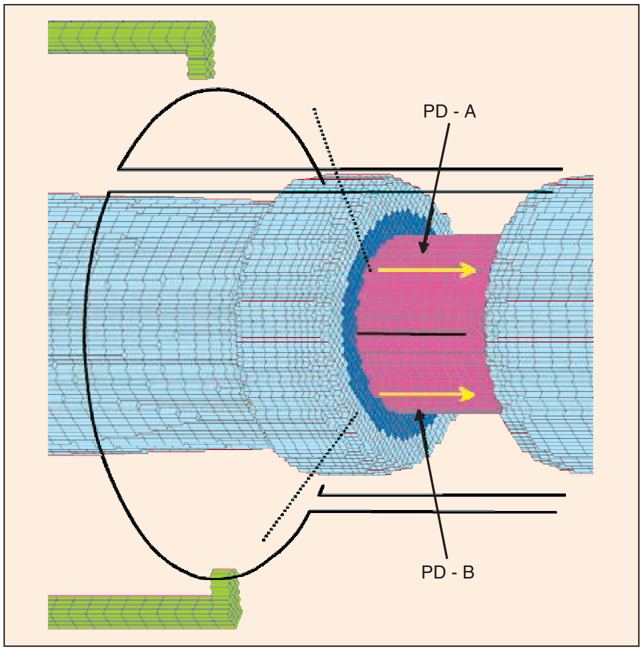

Figure 6. Two PD positions on the XLPE-silicone rubber interface shown relative to the sensor electrodes.

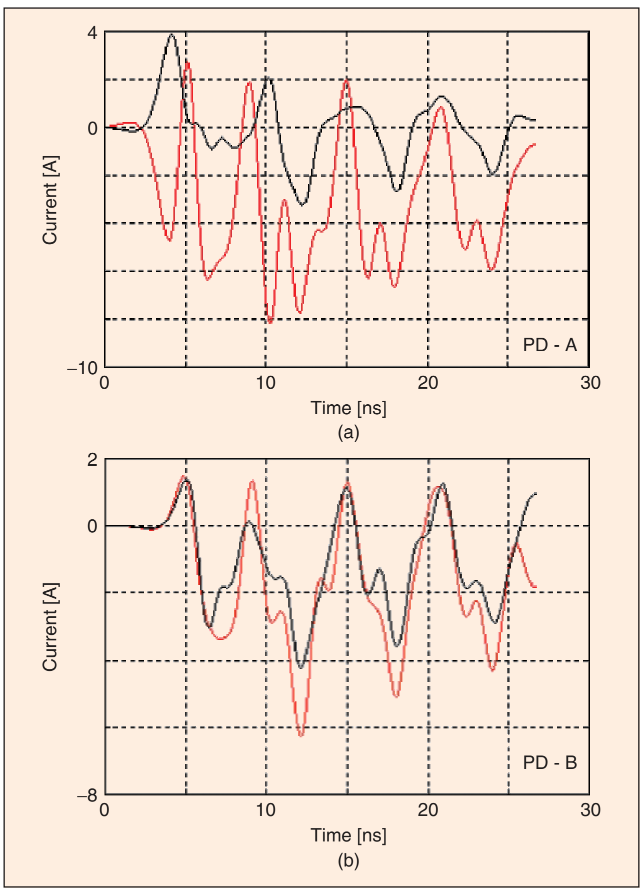

Figure 7. Output signals at the two electrodes for the topology shown in Fig. 6 for PD locations A and B. Differential amplification of the signals shown in the upper graph would result in a large signal. However, such amplification of the signals in the lower graph would result in a very small signal, which might be mistaken for the residual interference from a pulse propagating down the cable.

tion 1 is analyzed as shown in Fig. 8(b). Now a delay of 2.8 ns is computed. If one estimates the PD location based on this delay and the average propagation velocity, a location on the outer stress cone is obtained, although the PD is actually at the conductor shield, which shows that the cable joint is too complex for intuitive analysis.

Charge Estimation

In a standard PD measurement, the charge injected by the PD is measured from the low-frequency (e.g., 400 kHz) component, which provides effective integration of the PD pulse induced electromagnetic oscillations within the test system. Wideband PD detection improves the achievable signal-to-noise ratio [6]. Calibration of VHF PD measurement methods requires careful consideration, and in not every case can a calibration comparable to the standard low-bandwidth PD measurement be achieved. Typically, a pulse of known charge is injected into the high-voltage cable, and the peak voltage delivered by the sensor is measured. A meaningful calibration factor is obtained through the ratio of the injected charge to the peak voltage, as long as the injected pulse is narrow enough that the waveshape of the voltage at the sensor output is the impulse response of the sensor system. To obtain the data shown in Table II, the sensor concepts were calibrated as outlined above to obtain a calibration factor of pC/V. The PDs were then simulated inside the joint, and the charge they injected into the high-voltage cable was calculated (Table II, column 2).

To analyze how well the different sensors estimate these charges, the sensor output voltage was multiplied by a calibration factor to obtain the charge value. The largest value (by magnitude) was taken as the charge estimate. Table II normalizes these values to the charge injected into the high-voltage cable (columns 3-7) to obtain a relative charge error. Cells within the table with a relative charge error greater than 3 or less than 0.33 are shaded.

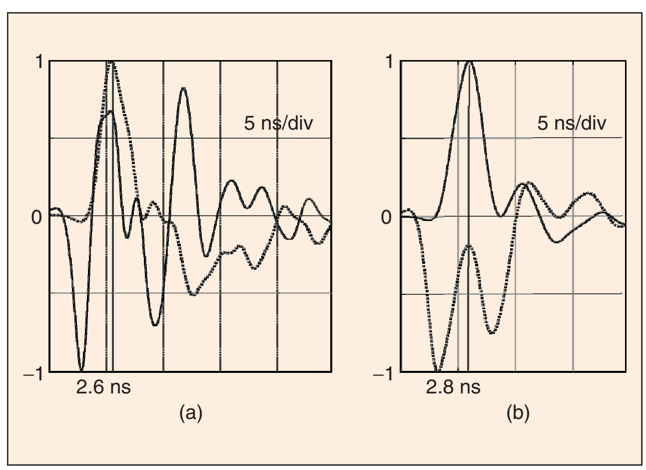

Figure 8. Currents to the left and right of the cable joint for PD at location 2(a) and 1(b) (Fig. 3). Currents are normalized to their peak values, as only the signal delay is of interest.

Table II. Relative Charge Error for the Sensor Concepts						
PD Loc.	Charge Injected into High-Voltage Cable	Charge Error Relative to the Charge in the High-Voltage Cable Configurations				
		E	D	B	A	C
1	2.2 pC	0.42	1.3	1.3	1.7	1.45
1x			1.3		0.45	
2	0.1 pC	2.9	20	25.9	113	24
2x			34.8		16.3	
3	1 pC	0.37	0.63	0.67	3	1.2
3x			0.63		0.06	
4	0.014pC	2.3	-4.5	-2.2	-5.4	-2
4x			-3		-0.6	

Only measurements taken at the cable (sensor configuration E) have errors of less than 3 for all PD locations investigated. In addition, all other methods estimate an incorrect polarity for PD location 4 (in some cases this was a near miss, as the positive and the negative peak values were of nearly the same magnitude). To investigate the influence of symmetry, PD locations have been moved by 90° or 180° relative to the PD sensor. Data for such sources are marked by an "x" in Table II.

All methods that attempted to suppress noise by taking the difference from two-sensor outputs (configurations A, C, and D) failed to detect PD in one or many PD locations. The only method that distinguished reliably between noise from the outside of the joint and PD from within the joint was the directional couplers attached to the cables (notwithstanding that other methods that attach sensors to the cable may also be as efficient and provide larger signals for certain PD locations).

Conclusions

This article shows that electromagnetic simulation can be applied to solve practical problems in high-voltage systems that involve complex geometries. Electromagnetic simulations help to select a PD sensor system to provide:

- optimal PD coupling in the desired frequency range
- the ability to distinguish between noise and PD
- good sensitivity for a wide range of PD locations.

Further applications of such simulations include PD detection and location in cable terminations, the pulse propagation in semi-shielded (e.g., concentric neutral) HV-cables, and PD and transient pulse propagation in SF_6-insulated apparatus, where much wider bandwidths are of concern as a result of the relatively small high-frequency attenuation of such systems. The next paper in this series will discuss the latter problem.

Acknowledgments

We are pleased to acknowledge the technical support of Dr. Weissenberg from Pirelli in Berlin, Germany (now with Brugg-Cables).

David Pommerenke received his diploma and Ph.D. from the Technical University Berlin while he was researching and teaching EMC and High Voltage. In 1996, he joined Hewlett Packard in Roseville, CA as an EMC engineer. In 2001, he accepted a position as Associate Professor in the EMC group at the University of Missouri-Rolla. His areas of interest are EMC, electrostatic discharge, numerical methods, and partial discharge detection. He can be reached at pommerenke@ece.umr.edu.

Roman Jobava was born in 1965 in Georgia, formerly in the U.S.S.R. He received his Ph.D. in radio-physics from Tbilisi State University, Tbilisi, Georgia, in 1990. Since 1991 he has been working at the Sukhumi Branch of Tbilisi State University and was appointed Associate Professor in 1996. From 1987 to 2000 he was a Senior Researcher in the Laboratory of Applied Electrodynamics, responsible for computer simulation of transient electromagnetic phenomena and development of appropriate numerical and software tools. In 2001 he began leading an Electromagnetic Consulting and Software Group. His research interests include numerical methods in applied electrodynamics, computer simulation of EMC problems, ESD, and transient field calculations. He may be reached at jobava@ieee.org.

Ralf Heinrich (1973) studied Electrical Engineering (High Frequency Engineering) at the Technical University of Berlin/Germany. He received his Dipl.-Ing. in Electrical Engineering in 1996 and his Dr.-Ing. in 2001. Since 1997 he has been working at the Institute for Electrical Power Engineering/High Voltage Engineering of the Technical University of Berlin in the field of PD measure-

ment techniques. He may be reached at rheinrich@ihs.ee.tu-berlin.de.

References

[1] D. Pommerenke and S. Sakaguchi, "Applications of Maxwell solvers to PD propagation—Part 1: Concepts and codes," *IEEE Electrical Insulation Magazine,* vol. 18, no. 5, pp. 15-21, 2002.

[2] R. Ross, "Dealing with interface problems in polymer cable terminations," *IEEE Electrical Insulation Magazine*, vol. 15, no. 4, pp. 5-9, Jul./Aug. 1999.

[3] C.G. Henningsen, K. Polster, B.A. Fruth, and D.W. Gross, "Experience with an on-line monitoring system for 400 kV XLPE cables," in *Proc. IEEE Power Eng. Soc. Trans. Distr. Conf.*, Los Angeles, CA, 1996, pp. 1099-1102.

[4] E. Pultrum and M.J.M. Van Riet, "HF partial discharge detection of HV extruded cable accessories," in *Proc. 1995 Jicable Conf.,* Versailles, France, 1995, pp. 662-665.

[5] D. Pommerenke, T. Strehl, R. Heinrich, W. Kalkner, F. Schmidt, and W. Weissenberg, "Discrimination between internal PD and other pulses using directional coupling sensors on high voltage cables," *IEEE Trans. Diel. Elect. Insul*, vol. 6, no.6, pp. 814-824, 1999.

[6] S.A. Boggs and G.C. Stone, "Fundamental limitations to the measurement of corona and partial discharge," *IEEE Trans. Elect. Insul.,* vol. EI-17, pp. 143-150, 1982.

[7] M.D. Judd and O. Farish, "Transfer functions for UHF partial discharge signals in GIS," in *Proc. Int. Symp. High Voltage (ISH)*, London, England, 1999, vol. 5, pp. 74-77.

[8] Parmigiani, Bruno, Lanfranconi, "Joint for cables with extruded insulation," US Patent 4,698,458, Oct. 6, 1987.

[9] D. Pommerenke, R. Jobava, and R. Heinrich, "Electromagnetic finite difference time domain (FDTD) modeling of partial discharge coupling applied to high voltage cables and cable joints," in *Proc. 8th IEE Int. Conf. Dielectric Materials, Measurements and Applications,* Edinburgh, U.K., 2000, pp. 497-502.

[10] G.C. Stone and S.A. Boggs, "Propagation of partial discharge pulses in shielded power cable," *1982 Annual Report Conf. Electrical Insulation Dielectric Phenomena (CEIDP),* 1982, pp. 275-280.

[11] R. Heinrich, S. Boenisch, D. Pommerenke, R. Jobava, and W. Kalkner, "Broadband measurement of the conductivity and the permittivity of semiconducting materials in high voltage XLPE cables," in *Proc. 8th IEE Int. Conf. Dielectric Materials, Measurements and Applications,* Edinburgh, U.K., 2000, pp. 123-234.

[12] Fidelity FDTD code from Zeland software, Version 1.2, Fremont, CA, USA.

[13] G. Katsuta, A. Toya, K. Muraoka, T. Endoh, Y. Sekii, and C. Ikeda, "Development of a method of partial discharge detection in extra-high voltage cross-linked polyethylene insulated cable lines," *IEEE Trans. Power Delivery*, vol. 7, no. 3, pp. 1068-79, 1992.